STRIP ADJUSTMENT USING CONJUGATE PLANAR AND LINEAR FEATURES IN OVERLAPPING STRIPS

Ana Paula Kersting
Ruifang Zhai
Ayman Habib
Dept. of Geomatics Engineering, University of Calgary, 2500 University Dr. NW,
Calgary, Alberta, T2N 1N4, Canada.
ana.kersting@ucalgary.ca
rzhai@geomatics.ucalgary.ca
habib@geomatics.ucalgary.ca

ABSTRACT

LiDAR (Light Detection And Ranging) technology has demonstrated its capabilities as a prominent technique for the acquisition of accurate topographic information with high-density. A LiDAR system consists of three main components: GPS, IMU, and laser units. Data collection is carried out in a strip-wise fashion and the ground coordinates of the laser footprints are derived using the direct geo-referencing information furnished by the onboard GPS/IMU. Due to systematic errors in the LiDAR components and/or alignment, adjacent LiDAR strips usually show discrepancies. Such discrepancies are caused by missing or improperly employed calibration and operational procedures. The ideal solution for the adjustment of neighboring strips is the implementation of an accurate calibration procedure. However, such a calibration demands the original observations (GPS, IMU and the laser measurements), which are not usually available to the end-user. In this work, a strip adjustment procedure for reducing or eliminating discrepancies between overlapping LiDAR strips is proposed. The mathematical model employed is similar to that used in the photogrammetric Block Adjustment of Independent Models (BAIM). Generally, a traditional BAIM uses conjugate points. These features, however, are not suitable for LiDAR surfaces since it is almost impossible to identify conjugate points in overlapping LiDAR strips. In this work, the use of planar patches and linear features, which are represented by sets of non-conjugate points, is investigated. The non-correspondence of the selected points along the planar and linear features is compensated for by artificially expanding their variance-covariance matrices. The paper presents experimental results from real data illustrating the feasibility of the proposed procedure.

INTRODUCTION

LiDAR has become a popular technology for the direct acquisition of topographic information. A LiDAR system integrates three main components: GPS, IMU, and laser units. The data collection is usually carried out in a strip-wise fashion where the ground coordinates of the laser footprints are derived using the measured ranges and the direct geo-referencing information furnished by the onboard GPS/IMU. The spatial and rotational offsets, which are known as the bore-sighting parameters, between the system's components are also needed for the computation of the ground coordinates of the laser footprints. The bore-sighting parameters together with other system parameters are derived through a calibration process, which is usually accomplished in several steps: (i) Laboratory calibration, (ii) Platform calibration, and (iii) In-flight calibration. In the laboratory calibration, which is conducted by the system manufacturer, the individual system components are calibrated. In addition, the eccentricity and misalignment between the laser mirror and the IMU as well as the eccentricity between the IMU and the sensor reference point are determined. In the platform calibration, the eccentricity between the sensor reference point and the GPS antenna is determined. The in-flight calibration utilizes a calibration test field composed of control surfaces for the estimation of the LiDAR system parameters. The observed discrepancies between the LiDAR-derived and control surfaces are used to refine the bore-sighting parameters and systematic errors in the system measurements (mirror angles and ranges). Current in-flight calibration methods have the following drawbacks: (i) They are time consuming and expensive; (ii) They are generally based on complicated and sequential calibration procedures; (iii) They require some effort for surveying the control surfaces; (iv) Some of the calibration methods involve manual and empirical procedures; (v) Some of the calibration methods require the availability of the LiDAR raw measurements such as ranges, mirror angles, as well as position and orientation information for each pulse (Filin, 2003; and Skaloud and

Lichti, 2006); and (vi) There is no commonly accepted methodology since the calibration techniques are usually based on a manufacturer-provided software package and the expertise of the LiDAR data provider. As a result of the non-transparent and sometimes empirical calibration procedures, collected LiDAR data might exhibit systematic discrepancies between conjugate surface elements in overlapping strips.

In the past few years, several methods have been developed for evaluating and/or improving LiDAR data quality by checking the compatibility of LiDAR footprints in overlapping strips (Kilian et al., 1996; Crombaghs et al., 2000; Maas, 2000; Bretar et al., 2004; Vosselman, 2004; Pfeifer et al., 2005). In Crombaghs et al. (2000), a method for reducing vertical discrepancies between overlapping strips is proposed. This approach does not deal with planimetric discrepancies, which might have larger magnitude when compared with vertical discrepancies. In Kilian et al. (1996), an adjustment procedure similar to the photogrammetric strip adjustment was introduced for detecting discrepancies and improving the compatibility between overlapping strips. The drawback of this approach is relying on distinct points to relate overlapping LiDAR strips and control surfaces. Due to the irregular nature of the LiDAR footprints, the identification of distinct points (e.g., building corners) is quite difficult and not reliable. More suitable primitives have been suggested by Maas (2000), where the correspondence is established between discrete points in one LiDAR strip and TIN patches in the other one. The correspondences are derived through a least-squares matching procedure where normal distances between conjugate point-patch pairs are minimized. This work focused on matching conjugate surface elements rather than improving the compatibility between neighbouring strips. Bretar et al., (2004) proposed an alternative methodology for improving the quality of LiDAR data using derived surfaces from photogrammetric procedures. The main disadvantage, which limits the practicality of this methodology, is relying on having aerial imagery over the same area. In Pfeifer et al. (2005) and Vosselman (2004), other methods were developed for detecting discrepancies between overlapping strips.

The main objective of this paper is to present a new procedure for the strip adjustment while utilizing appropriate primitives that can be extracted from the LiDAR data with a satisfactory level of automation (i.e., requiring minimum user interaction). The paper starts with a brief discussion of the LiDAR mathematical model, which is followed by an analysis of some of the systematic errors and their impact on the resulting surface. Then, the proposed procedure for the strip adjustment, including the extraction and matching of the appropriate primitives, is presented. The performance of the proposed strip adjustment procedure is evaluated through experimental results from real data. Finally, the paper presents some conclusions and recommendations for future work.

LiDAR MATHEMATICAL MODEL

The coordinates of the LiDAR footprints are the result of combining the derived measurements from each of its system components, as well as the bore-sighting parameters relating such components. The relationship between the system measurements and parameters is embodied in the LiDAR equation (Vaughn et al., 1996; Schenk, 2001; El-Sheimy et al., 2005), Equation 1. As it can be seen in Figure 1, the position of the laser footprint, $\vec{X}_G$, can be derived through the summation of three vectors ($\vec{X}_o, \vec{P}_G$ and $\vec{\rho}$) after applying the appropriate rotations: $R_{yaw,\ pitch,\ roll}$, $R_{\Delta\omega,\Delta\phi,\Delta\kappa}$ and $R_{\alpha,\beta}$. In this equation, $\vec{X}_o$ is the vector from the origin of the ground coordinate system to the origin of the IMU coordinate system, $\vec{P}_G$ is the offset between the laser unit and IMU coordinate systems (bore-sighting offset), and $\vec{\rho}$ is the laser range vector whose magnitude is equivalent to the distance from the laser firing point to its footprint. The term $R_{yaw,\ pitch,\ roll}$ stands for the rotation matrix relating the ground and IMU coordinate systems, $R_{\Delta\omega,\Delta\phi,\Delta\kappa}$ represents the rotation matrix relating the IMU and laser unit coordinate systems (angular bore-sighting), and $R_{\alpha,\ \beta}$ refers to the rotation matrix relating the laser unit and laser beam coordinate systems with α and β being the mirror scan angles. For a linear scanner, which is the focus of this paper, the mirror is rotated in one direction only leading to zero α angle. The involved quantities in the LiDAR equation are all measured during the acquisition process except for the bore-sighting angular and offset parameters (mounting parameters), which are usually determined through a calibration procedure.

$$\vec{X}_G = \vec{X}_o + R_{yaw,\,pitch,\,roll}\ \vec{P}_G + R_{yaw,\,pitch,\,roll}\ R_{\Delta\omega,\,\Delta\phi,\,\Delta\kappa}\ R_{\alpha,\,\beta} \begin{bmatrix} 0 \\ 0 \\ -\rho \end{bmatrix} \quad (1)$$

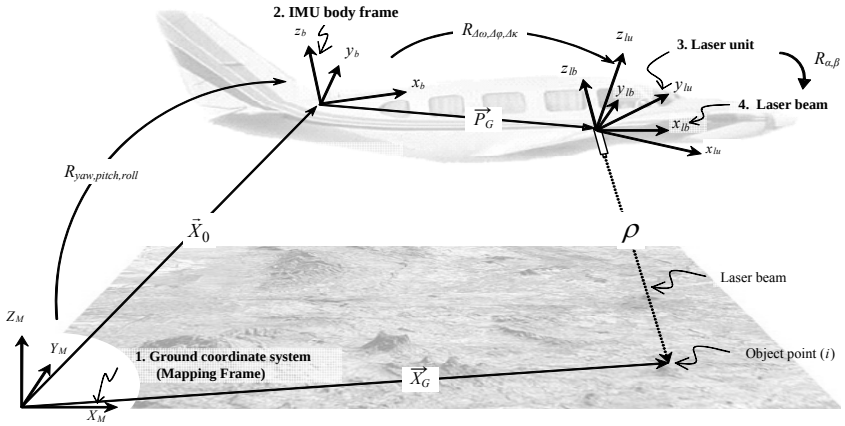

Figure 1. Coordinate systems and involved quantities in the LiDAR equation.

LiDAR ERROR BUDGET

The quality of the derived point cloud from a LiDAR system depends on the random and systematic errors in the system measurements and parameters. A detailed description of LiDAR random and systematic errors can be found in Huising and Pereira (1998), Baltsavias (1999), and Schenk (2001). The magnitude of the random errors depends on the accuracy of the system's measurements, which include position and orientation measurements from the GPS/INS, mirror angles, and ranges. Systematic errors, on the other hand, are mainly caused by biases in the bore-sighting parameters relating the system components as well as biases in the system measurements (e.g., ranges and mirror angles). As a strip adjustment procedure is concerned with minimizing the impact of systematic errors in the LiDAR system on the derived point cloud, it is mandatory to understand the nature and impact of possible systematic errors in a LiDAR system.

The systematic errors effect will be derived through a simulation process starting from a given surface and trajectory, which are then used to derive the system measurements (ranges, mirror angles, position and orientation information for each pulse). Then, biases are added to the system parameters, which are used to reconstruct the surface through the LiDAR equation. The differences between the bias-contaminated and true coordinates of the footprints within the mapped area are used to represent the impact of a given bias in the system parameters or measurements. In this work, the impact of biases in the bore-sighting offset parameters and bore-sighting angular parameters is investigated. The following conclusions could be drawn from the simulation experiments:

- **Bore-sighting offset parameters**: the biases in the bore-sighting offset parameters will lead to constant shifts in the derived point cloud. The shifts in the XY-directions are dependent on the flying direction. The shift in the Z-direction, on the other hand, is independent of the flying direction. Moreover, the planimetric and vertical shifts are independent of the flying height and scan angle. The differences between the reconstructed LiDAR footprints and the simulated surface (control), for two overlapping strips flown in opposite directions after the introduction of the bore-sighting offset biases, are illustrated in Figure 2a. For two strips flown in opposite directions, biases in the planimetric bore-sighting offsets will cause constant discrepancies between conjugate features in the planimetric directions. For two strips flown in the same direction, on the other hand, bore-sighting offset biases will not cause any discrepancy between conjugate features, since the effect will be the same for both strips. Moreover, no discrepancy will be detected between conjugate features in the vertical direction. We can observe that for strips flown in opposite directions (refer to Figure 2a), averaging the spatial coordinates will cancel out the effect of planimetric bore-sighting biases.

- **Bore-sighting angular parameters:**
  (a) *Pitch bias*: the pitch bias will cause a constant shift along the flight direction, whose effect is dependent on the flying direction. The differences between the reconstructed LiDAR footprints after the introduction of the bore-sighting pitch bias and the simulated surface (control) for two overlapping strips flown in opposite directions are illustrated in Figure 2b. The discrepancy between conjugate features in overlapping strips will be dependent on the strip's flight direction. For two strips flown in the same direction, bore-sighting pitch bias will not cause any discrepancy between conjugate features, since the effect will be the same for both strips. Conversely, for two strips flown in opposite directions, bore-sighting pitch bias will cause constant discrepancy between conjugate features in the along-flight direction. No discrepancy will be detected between conjugate features in the across flight and vertical directions. It can be noticed that for strips flown in opposite directions, averaging the spatial coordinates will cancel out the effect of the bore-sighting pitch bias.

  (b) *Roll bias*: the bore-sighting roll bias will cause a constant shift across the flight direction and a shift in the Z direction with magnitude varying linearly across the flying direction. Both effects are dependent on the flying direction. The differences between the reconstructed LiDAR footprints after the introduction of the bore-sighting roll bias and the simulated surface (control) for two overlapping strips flown in opposite directions are shown in Figure 2c. In terms of discrepancies between overlapping strips, if the strips are flown in the same direction, bore-sighting roll bias will only cause constant vertical discrepancy between conjugate features. For two strips flown in opposite directions, a constant discrepancy will be detected between conjugate features in the across-flying direction and a discrepancy with linearly varying magnitude will be detected between conjugate features in the vertical direction, which is equivalent to the effect of a rotation across the flight direction. Moreover, no discrepancy will be detected between conjugate features in the along flying direction. For strips flown in opposite directions (refer to Figure 2c), averaging the spatial coordinates will cancel out the planimetric effect of the bore-sighting roll bias. Only for strips with 100% side lap that are flown in opposite directions, averaging the spatial coordinates will cancel out the vertical effect of bore-sighting roll bias. For strips flown in the same or opposite directions, averaging the spatial coordinates will reduce the vertical deviation from the true surface.

  (c) *Yaw bias*: the effect of the bore-sighting yaw bias on the derived LiDAR footprints is only a shift along the flying direction with magnitude varying linearly across the flight direction. This effect is independent of the flying direction. The differences between the reconstructed LiDAR footprints after the introduction of the bore-sighting yaw bias and the simulated surface (control) for two overlapping strips flown in opposite directions are shown in Figure 2d. For two strips flown in the same or opposite directions, bore-sighting yaw bias will only cause a constant discrepancy between conjugate features in the along flight direction. No discrepancy will be detected between conjugate features in the across flight direction and in the vertical direction. For two strips flown with 100% overlap no discrepancy will be observed. For strips flown in the same or opposite directions, averaging the spatial coordinates will not cancel out the effect of bore-sighting heading bias. Averaging the spatial coordinates will, however, reduce the deviation from the true surface.

In summary, the discrepancies caused by the bore-sighting offset and angular biases can be modeled by shifts and a rotation across the flight direction. Therefore, a six-parameter rigid-body transformation (three shifts and three rotations) is sufficient for modeling the introduced discrepancies by biases in the bore-sighting parameters in overlapping strips. Having discussed the impact of systematic errors, the focus will be shifted towards the strip adjustment procedure.

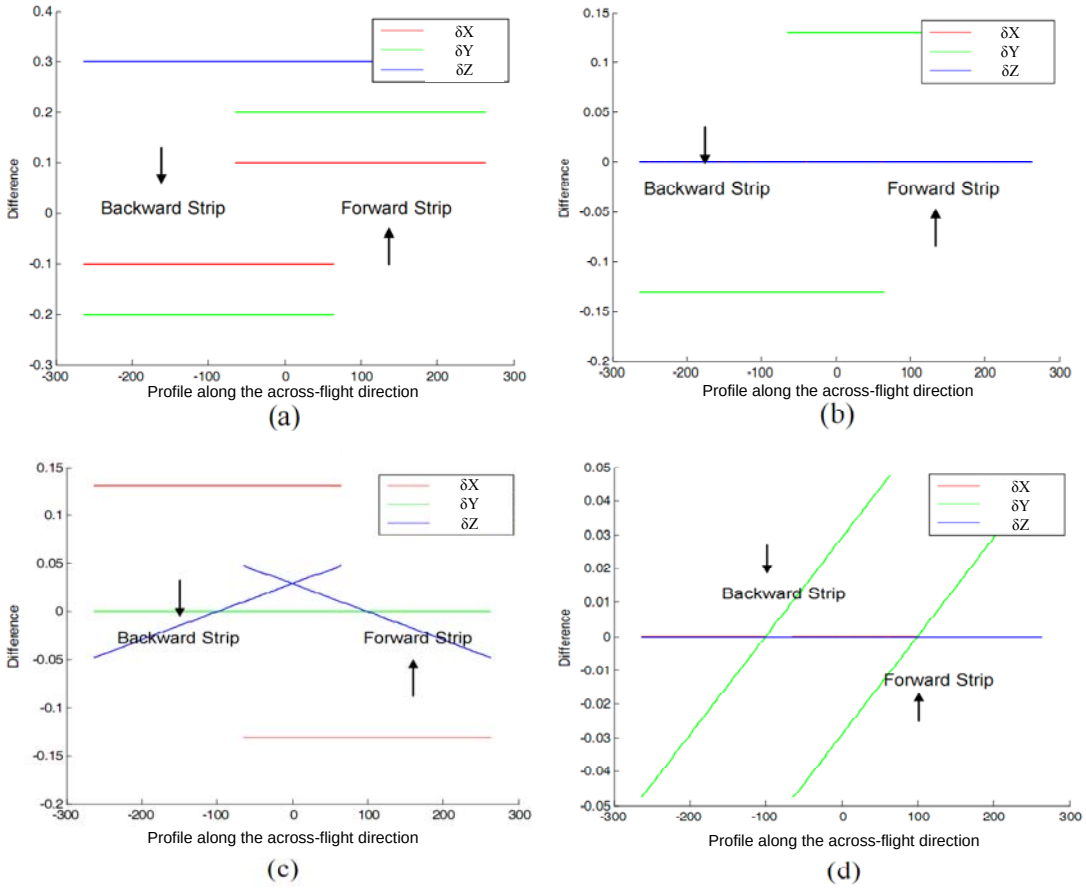

Figure 2. Differences between the bias-contaminated and true locations of the footprint for two overlapping strips, which are flown in opposite directions, after the introduction of bore-sighting offset biases (a), bore-sighting pitch bias (b), bore-sighting roll bias (c), and bore-sighting yaw bias (d).

STRIP ADJUSTMENT

The main goal of strip adjustment is to minimize the impact of systematic errors in the LiDAR system parameters by improving the compatibility among neighbouring strips. In addition, the estimated transformation parameters relating overlapping strips can be used to verify the quality of the system calibration. In the absence of biases in the system parameters, overlapping strips should coincide with each other without the need for any shifts or rotations. In other words, significant deviations from zero shifts and rotations can be used as an indication of the presence of systematic errors in the data acquisition system. Improving the compatibility between neighbouring strips can be viewed as the co-alignment of the different strips to a common reference frame. Therefore, the strip adjustment can be thought of as a registration procedure. An effective registration process should deal with four main issues: the registration primitives, establishing the correspondence between conjugate primitives, the transformation function relating the reference frames of the involved datasets, and the similarity measure which utilizes conjugate primitives for the estimation of the involved parameters in the transformation function. As it has been mentioned in the previous section, a six-parameter rigid-body transformation can be used as the transformation function relating overlapping strips in the presence of biases in the bore-sighting parameters. Traditional registration procedures (e.g., photogrammetric Block Adjustment of Independent Models – BAIM) are usually based on point primitives. These primitives, however, are not suitable when dealing with LiDAR data since it is quite difficult to establish the correspondence between distinct points in the irregularly-distributed footprints. Therefore, the use of planar patches and linear features is proposed in this work. In the following sub-sections, the extraction and matching of primitives will be described. Also, the similarity measure, which incorporates the extracted primitives for the estimation of the parameters of the transformation function, will be presented.

Primitives Extraction and Matching

In this section, the developed environment for the extraction of areal and linear features in overlapping strips is introduced. These primitives are extracted from the irregular LiDAR footprints. The process starts by displaying the LiDAR intensity images for overlapping strips where the operator selects an area where areal and linear features might exist. The user clicks on the centre of the area after defining the radius of a circle, within which the original LiDAR footprints will be extracted. It should be noted that the LiDAR intensity images are only used for visualization purposes. The user needs to establish the area of interest in one of the strips and the corresponding areas in the other strips are automatically defined. Figure 3a shows the specified area in one of the strips as well as the original LiDAR footprints in that area. Then a segmentation technique (Kim et al., 2007) is used to identify planar patches in the point cloud within the selected area. This segmentation procedure is independently run on the point cloud for all the overlapping strips. The outcome from such segmentation is aggregated sets of points representing planar patches in the selected area, Figure 3b. For linear features extraction, neighbouring planar patches are identified and intersected to produce straight-line segments, Figure 3c. This procedure is repeated for several areas within the overlap portion in the involved strips.

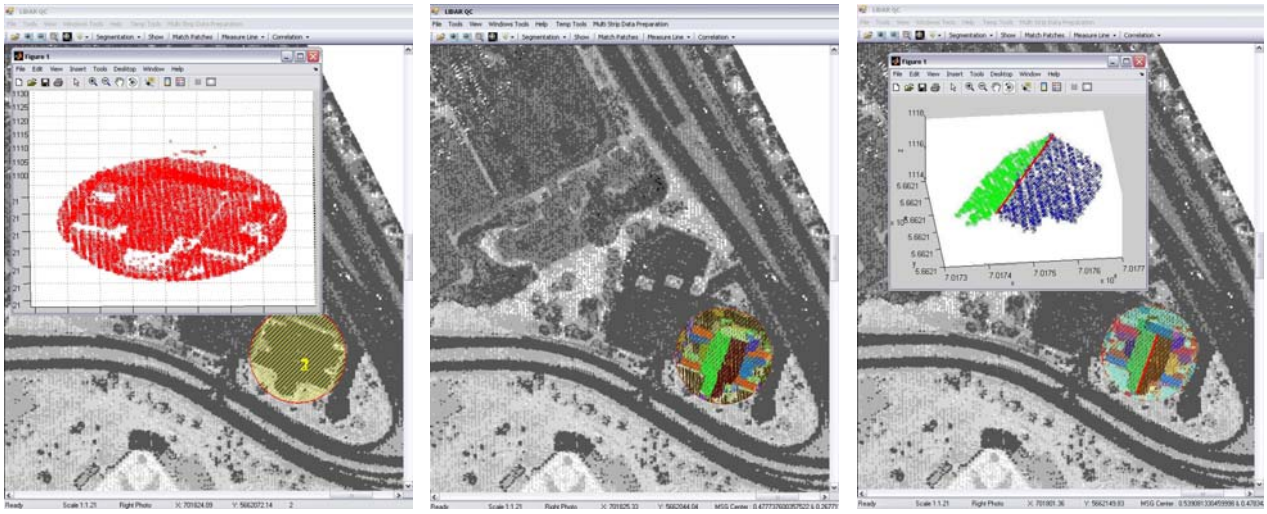

(a) (b) (c)

Figure 3. Area of interest selection and LiDAR point cloud extraction (a), segmented planar patches (b), and extracted linear features in the area of interest (c).

The outcome of the extraction procedure is a set of linear and areal features in overlapping strips. Due to the nature of the LiDAR data acquisition (e.g., scan angle, surface normal, surface reflectivity, occlusions), there is no guarantee that there is one-to-one correspondence between the extracted primitives from overlapping strips. To solve the correspondence problem, one has to utilize the attributes of the extracted primitives. For example, conjugate planar patches can be matched by checking the distance between the respective centroids and the parallelism of their surface normal (Figure 4a). On the other hand, conjugate linear features can be automatically matched using the normal distance, parallelism, and the percentage of overlap between candidate lines in overlapping strips (Figure 4b). A graphic visualization of matched planar and linear features is presented to the user for final confirmation of the validity of the matched primitives. Having extracted conjugate patches and linear features from overlapping strips, the focus will be shifted towards using these primitives for the estimation of the parameters of the transformation functions relating these strips.

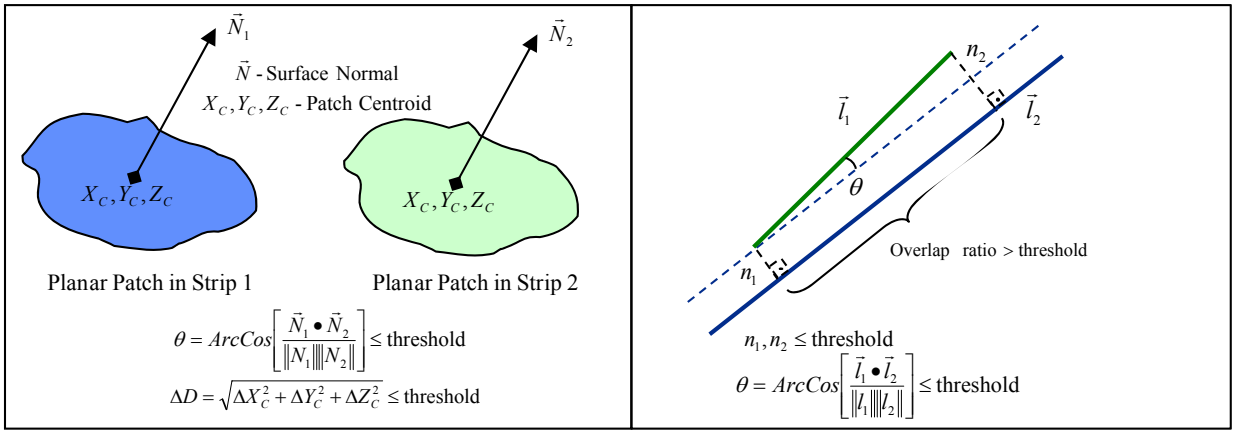

Figure 4. Matching of conjugate patches (a) and conjugate linear features (b) in overlapping strips.

Similarity Measure

So far, a semi-automated approach for the extraction of areal and linear features from overlapping strips was presented. The extracted primitives are then matched using their respective attributes. In this section, the similarity measure, which incorporates the matched primitives together with the established transformation function to mathematically describe their correspondence, is introduced. The formulation of the similarity measure depends on the representation scheme for the involved primitives. In this work, an areal feature will be represented by its centroid together with the orientation of its surface normal. A linear feature, on the other hand, will be represented by its end points. It should be noted that the points representing corresponding areal and linear features are not necessarily conjugate to each other. In this research, a point-based similarity measure, which can deal with non-conjugate points, is proposed. More specifically, a rigid body transformation (Equation 2) will be used to relate the observed strip coordinates (X_S, Y_S, Z_S) to the adjusted strip coordinates ($X_{S_A}, Y_{S_A}, Z_{S_A}$). Such a transformation will minimize the inconsistency among overlapping strips. The adjusted strip coordinates together with the parameters of the transformation function for the involved strips will be estimated through a Least Squares Adjustment (LSA) procedure.

$$\begin{bmatrix} X_S \\ Y_S \\ Z_S \end{bmatrix} = \begin{bmatrix} X_T \\ Y_T \\ Z_T \end{bmatrix} + R_{\omega,\phi,\kappa} \begin{bmatrix} X_{S_A} \\ Y_{S_A} \\ Z_{S_A} \end{bmatrix} \tag{2}$$

In order to compensate for fact that the observed points along corresponding features in overlapping strips are not conjugate, one can manipulate the variance-covariance matrices Σ_{XYZ} for such points. For the centroid of a planar feature, the variance of that point along the plane will be expanded. In a similar fashion, the variance of the points defining the linear feature will be expanded along the line direction. To illustrate the variance expansion procedure, one can consider the case for a point representing the centroid of an areal feature. First, a local coordinate system (*UVW*) with the *U* and *V* axes aligned along the plane is defined. The relationship between the strip coordinate system (*XYZ*) and the local coordinate system (*UVW*) can be represented by Equation 3. The rotation matrix in that equation is defined using the orientation of the normal to the planar patch including the point in question. The variance-covariance matrix Σ_{XYZ}, shown in Equation 4, depends on the accuracy specification of the data acquisition system. Using the law of error propagation, the variance of that point in the local coordinate system Σ_{UVW} can be derived according to Equation 5. The variances are expanded along the plane parallel direction by introducing large numbers in the matrix components corresponding to the *U* and *V* axes (Equation 6). Finally, the variance-covariance matrix Σ'_{XYZ} in the original coordinate system can be derived according to Equation 7. When dealing with linear features, Equations 3 – 7 can be used while replacing Equation 6 with Equation 8 (where the variance is only expanded along the line direction).

$$\begin{bmatrix} U \\ V \\ W \end{bmatrix} = R \begin{bmatrix} X \\ Y \\ Z \end{bmatrix} \tag{3}$$

$$\sum_{XYZ} = \begin{bmatrix} \sigma_X^2 & \sigma_{XY} & \sigma_{XZ} \\ \sigma_{YX} & \sigma_Y^2 & \sigma_{YZ} \\ \sigma_{ZX} & \sigma_{ZY} & \sigma_Z^2 \end{bmatrix} \tag{4}$$

$$\sum_{UVW} = R \sum_{XYZ} R^T \tag{5}$$

$$\text{For planar patches} \rightarrow \sum\nolimits'_{UVW} = \sum_{UVW} + \begin{bmatrix} N & 0 & 0 \\ 0 & M & 0 \\ 0 & 0 & 0 \end{bmatrix}, \quad \text{where N and M are large numbers} \tag{6}$$

$$\sum\nolimits'_{XYZ} = R^T \sum\nolimits'_{UVW} R \tag{7}$$

$$\text{For lines} \rightarrow \sum\nolimits'_{UVW} = \sum_{UVW} + \begin{bmatrix} N & 0 & 0 \\ 0 & 0 & 0 \\ 0 & 0 & 0 \end{bmatrix}, \quad \text{where N is a large number} \tag{8}$$

EXPERIMENTAL RESULTS

The experimental results section aims at testing the validity of the presented procedure using a real dataset as well as exploring the impact of such an adjustment procedure.

Dataset Description

To evaluate the performance of the proposed methodology, a real LiDAR dataset was acquired. The dataset was captured in two different mapping missions, which were 42-days apart, with the same system using two aircrafts. In the first day of data collection, six strips with 50% overlap were collected from a flying height of 1,000m (Figure 5a). In the second day, four strips covering the same region but with a smaller overlap ratio were captured from a flying height of 1,400m (Figure 5b). The flight configurations and the accuracy specifications for these flights are listed in Table 1. All neighbouring strips were captured from almost parallel flight lines in opposite directions.

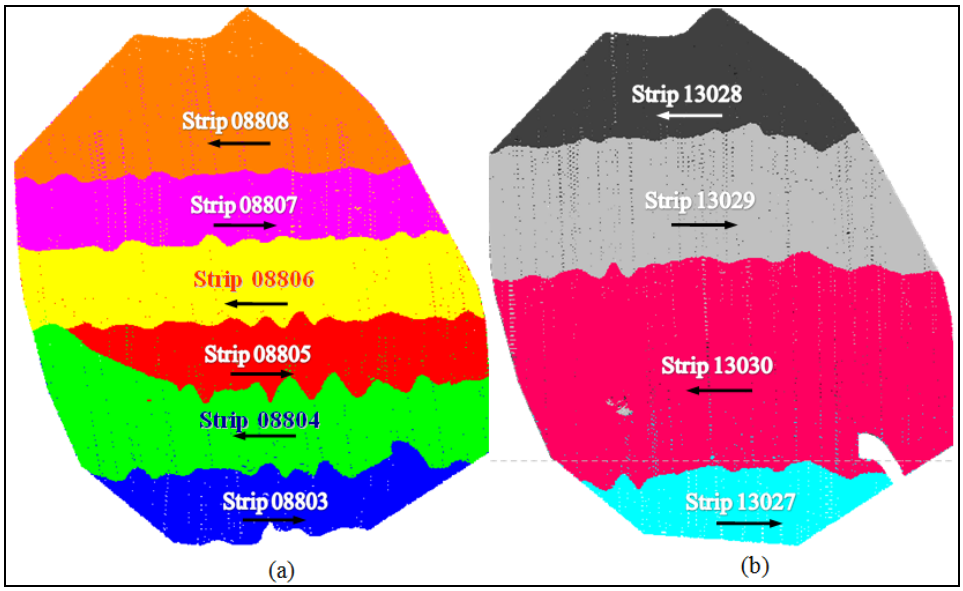

Figure 5. Area coverage of the six flight lines in the first mapping mission, Julian Day 88 (a) and the four strips in the second mapping missions, Julian Day 130 (b).

Table 1. System and flight specifications for the strips in Figure 5

Sensor Model	Optech 3100
Flying Height	≈ 1000 & 1400m
Ground Point Spacing	≈ 0.75m
Vertical Accuracy	≈ 15 cm
Horizontal Accuracy	≈ 50cm@1000m
	≈ 70cm@1400m
2 Surveying Days	
– 1st Day: 088	6 strips @1000m
– 2nd Day: 130	4 strips @1400m

Strip Adjustment Results

The proposed semi-automated procedure for the extraction and matching of corresponding linear and areal features has been applied leading to the identification of forty-eight planar patches and forty-two linear features in the ten strips. These features are identified in as many strips as possible. The points representing these features, after the variance expansion, are then used in a LSA procedure to estimate the transformation parameters for the involved strips as well as the adjusted strip coordinates. The estimated transformation parameters using planar and linear features are listed in Table 2. A closer look at this table reveals the following:

1. Significant differences from the expected zero shifts and rotations indicate the presence of biases in the system bore-sighting parameters.
2. The most significant deviation is observed in the X-direction (refer to the X_T values in Table 2). Such a deviation can be the result of biases in the bore-sighting pitch and heading angles.
3. The least deviation from the optimum values is observed in the Z-direction (refer to the Z_T values in Table 2). These observations confirm the prior expectation of more significant impact of biases in bore-sighting parameters on the planimetric coordinates when compared with their impact on the vertical coordinates.

Table 2. Estimated transformation parameters using conjugate planar patches in overlapping strips

Strip	Measured Patches	Measured Lines	X_T (m)	Y_T (m)	Z_T (m)	ω (^{0})	φ (^{0})	κ (^{0})
8803	26	12	-0.98	0.12	0.03	-0.0001	-0.0002	0.0022
8804	30	19	-0.81	-0.09	0.00	-0.0003	0.0000	-0.0074
8805*	41	40	**0**	**0**	**0**	**0**	**0**	**0**
8806	30	32	0.02	-0.07	-0.03	-0.0003	-0.0004	0.0068
8807	36	18	0.99	-0.09	0.04	0.0001	-0.0013	0.0135
8808	18	14	1.20	-0.17	0.03	-0.0001	-0.0013	0.0179
13027	12	6	-1.99	0.00	0.08	0.0002	-0.0013	0.0051
13028	18	13	1.44	-0.09	0.01	0.0000	-0.0008	0.0122
13029	29	28	-0.08	-0.07	0.03	0.0000	-0.0005	-0.0036
13030	18	17	-0.51	0.07	0.01	0.0003	-0.0004	0.0032

***Reference Strip**

The improvement in the strips' compatibility after the strip adjustment procedure can be observed in the profile shown in Figure 6. The surface shown in this profile is tilted with the aspect almost parallel to the flight direction, which is the direction where the most significant discrepancy takes place (refer to the X_T values in Table 2). A subjective evaluation of the impact of the strip adjustment was also conducted by inspecting the generated intensity images (Figure 7). As it can be seen in this figure, enhancement in the feature definition, such as at buildings' edges and pavement markings, is visible in the generated intensity images after the strip adjustment (refer to the circled areas in Figure 7). It is also obvious that the enhancement is more visible for features, which are almost perpendicular to the flight direction. Once again, such an enhancement should be expected since the observed discrepancies among overlapping strips take place along the flight direction.

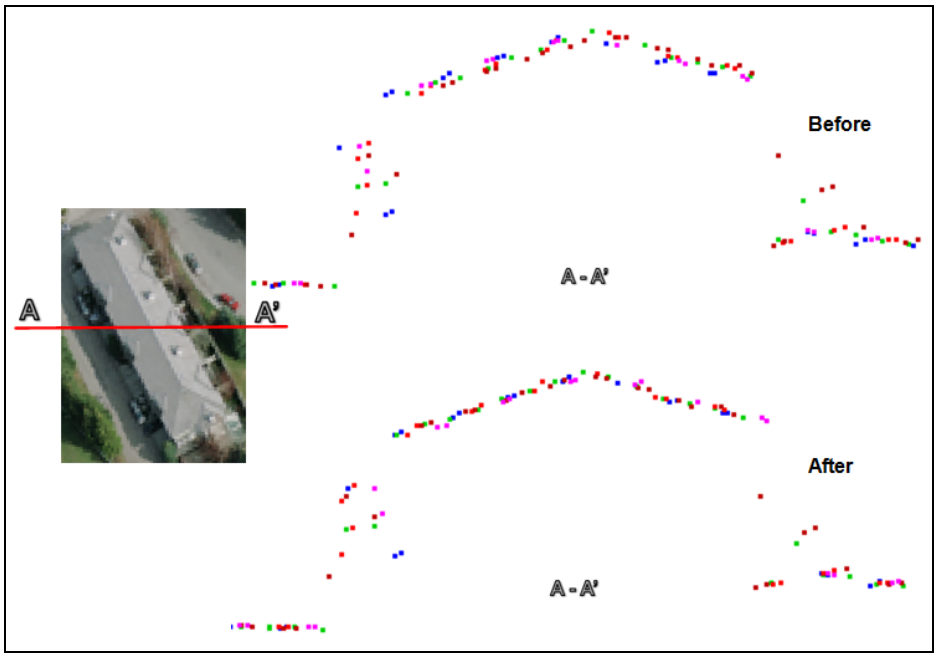

Figure 6. Profile along the flight direction crossing a tilted surface before (a) and after (b) the strip adjustment.

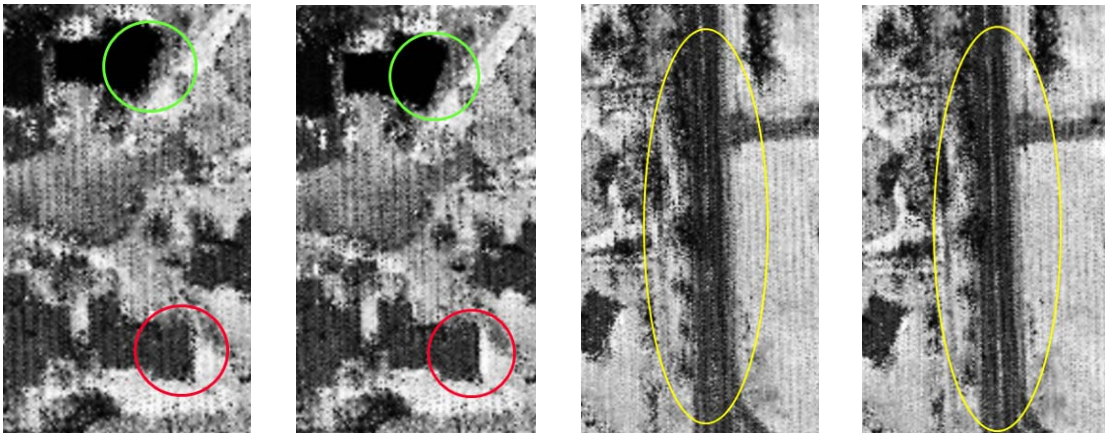

(a) (b) (c) (d)

Figure 7. Intensity images with highlighted buildings' edges before (a) and after (b) the strip adjustment, and intensity images with highlighted pavement markings before (c) and after (d) the strip adjustment.

One should note that the presented strip adjustment procedure mainly aims at improving the alignment between the strips and this does not necessarily mean improving the alignment of the adjusted strips relative to the ground coordinate system. In other words, one of the strips is chosen to be as a reference strip and the remaining strips are aligned relative to that strip, which is not bias free. As discussed in the error budget section, for strips flown in opposite direction with 50%, overlap a simple averaging process will lead to a surface which is closer to the ground truth and a strip adjustment procedure is not recommended in this case. For example, the planimetric biases introduced by systematic errors in the spatial bore-sighting parameters as well as the bore-sighting pitch and roll angles will be cancelled out by averaging the LiDAR data in overlapping strips. The impact of a bore-sighting yaw bias (Figure 2d), however, will not be completely cancelled out by the averaging process. However, for such a bias, the impact will be partially reduced.

CONCLUSIONS

The direct acquisition of a high density and accurate 3D point cloud has made LiDAR systems the preferred technology for the generation of topographic data to satisfy the needs of several applications (e.g., digital surface model creation, digital terrain model generation, orthophoto production, 3D city modeling, and forest mapping). The non-transparent and sometimes empirical calibration procedures, however, might lead to consistent discrepancies between conjugate surface elements in overlapping strips. This paper presented a procedure to improve the compatibility among overlapping strips. First, the impact of systematic errors in the bore-sighting parameters on the derived point cloud is investigated. Such an investigation proved that conjugate surface elements in overlapping strips can be related through a rigid-body transformation (three shifts and three rotations). Then, a semi-automated approach for the extraction and matching of conjugate linear and areal features in overlapping strips was introduced. The extracted features are represented by a set of non-conjugate points. The established transformation function and the matched primitives were used to estimate the necessary transformation parameters for the best co-alignment of the LiDAR strips. The non-correspondence of the selected points along the planar and linear features is compensated for by artificially expanding their variance-covariance matrices. Other than the co-alignment of overlapping strips, the developed procedure can be used to infer the presence of systematic errors in the data acquisition system. For an accurately calibrated LiDAR system, no shifts and rotations are needed to improve the compatibility of overlapping strips. Deviations from zero shifts and rotation can be used for the quality control the LiDAR system and derived data.

The performance of the proposed procedure was evaluated using real datasets. The experimental results revealed that the strip adjustment would improve the strips' compatibility and as a consequence the visual appearance of the generated intensity images from multiple strips. In conclusion, one should note that the best way to improve the compatibility among overlapping strips is by implementing a rigorous calibration procedure. As far as the positioning accuracy is concerned, flying in opposite strips with 50% overlap will minimize the impact of the discussed biases in this paper without the need for strip adjustment as long as an averaging procedure is utilized to derive feature locations.

ACKNOWLEDGEMENT

We would like to thank the GEOIDE (GEOmatics for Informed DEcisions) Network of Centers of Excellence of Canada for their financial support of this research (SII#43). The authors are also indebted to the University of Calgary - Information Technology for providing the LIDAR/image data and the valuable feedback.

REFERENCES

Baltsavias, E., 1999. Airborne laser scanning: existing systems and firms and other resources, *ISPRS Journal of Photogrammetry and Remote Sensing*, 54 (2-3): 164-198.

Bretar F., M. Pierrot-Deseilligny, and M. Roux, 2004. Solving the strip adjustment problem of 3D airborne lidar data, *Proceedings of the IEEE IGARSS'04,* 20-24 September, Anchorage, Alaska.

Crombaghs, M., E. De Min, and R. Bruegelmann, 2000. On the adjustment of overlapping strips of laser altimeter height data, *International Archives of Photogrammetry and Remote Sensing*, 33(B3/1): 230-237.

El-Sheimy, N., C. Valeo, and A. Habib, 2005. *Digital Terrain Modeling: Acquisition, Manipulation and Applications*, Artech House Remote Sensing Library, 257 p.

Filin, S., 2003. Recovery of systematic biases in laser altimetry data using natural surfaces, *Photogrammetric Engineering and Remote Sensing*, 69(11):1235–1242.

Huising, E. J., and L. M. G. Pereira, 1998. Errors and accuracy estimates of laser data acquired by various laser scanning systems for topographic applications, *ISPRS J. of Photogrammetry and Remote Sensing*, 53(5): 245-261.

Kilian, J., N. Haala, and M. Englich, 1996. Capture and evaluation of airborne laser scanner data, *International Archives of Photogrammetry and Remote Sensing*, 31(B3):383–388.

Kim C., Habib A., Mrstik P., 2007. New approach for planar patch segmentation using airborne laser data, *Proceedings of the ASPRS 2007 Annual Conference*, Tampa, Florida.

Maas, H. G., 2000. Least-squares matching with airborne laserscanning data in a TIN structure, *International Archives of Photogrammetry and Remote Sensing*, 33(B3/1): 548-555.

Pfeifer, N., S. O. Elberink, and S. Filin, 2005. Automatic tie elements detection for laser scanner strip adjustment, *International Archives of Photogrammetry and Remote Sensing*, 36(3/W3): 1682-1750.

Schenk, T., 2001. Modeling and Analyzing Systematic Errors in Airborne Laser Scanners, Technical Report in Photogrammetry No. 19, Ohio Sate University.

Skaloud, J. and D. Lichti, 2006. Rigorous approach to bore-sight self-calibration in airborne laser scanning, *ISPRS Journal of Photogrammetry and Remote Sensing*, 61: 47–59.

Vaughn, C. R., J. L. Bufton, W. B. Krabill, and D. L. Rabine, 1996. Georeferencing of airborne laser altimeter measurements, *International Journal of Remote Sensing*, 17(11): 2185-2200.

Vosselman, G., 2004. Strip Offset Estimation Using Linear Features, http://www.itc.nl/personal/vosselman/papers/vosselman2002.columbus.pdf (last accessed: 15 November 2007).